Contrast adaptation reveals increased organizational complexity of chromatic processing in the visual evoked potential

Chad S. Duncan,[1,*] Eric J. Roth,[1] Yoko Mizokami,[2] Kyle C. McDermott,[1] and Michael A. Crognale[1]

[1]Department of Psychology, University of Nevada, Reno 0296, 1664 N. Virginia Street, Reno, Nevada 89557, USA
[2]Graduate School of Advanced Integration Science, Chiba University, Optic1-33 Yayoicho,
Inage-ku, Chiba 263-8522, Japan
**Corresponding author: cduncan@unr.edu*

Received September 2, 2011; revised November 22, 2011; accepted November 25, 2011;
posted November 28, 2011 (Doc. ID 153976); published January 25, 2012

Results from psychophysics and single-unit recordings suggest that color vision comprises multiple stages of processing. Postreceptoral channels appear to consist of both a stage of broadly tuned opponent channels that compare cone signals and a subsequent stage, which includes cells tuned to many different directions in color space. The chromatic visual evoked potential (crVEP) has demonstrated chromatic processing selective for cardinal axes of color space. However, crVEP evidence for higher-order color mechanisms is lacking. The present study aimed to assess the contribution of lower- and higher-order color mechanisms to the crVEP by using chromatic contrast adaptation. The results reveal the presence of mechanisms tuned to intermediate directions in color space in addition to those tuned to the fundamental cardinal axes. © 2012 Optical Society of America

OCIS codes: 330.1720, 330.4270, 330.7320, 330.1800.

1. INTRODUCTION

Psychophysical and physiological research has shown that color processing is divided into multiple distinct stages [1]. The first begins with the activation of the three cone types, L, M, and S, which each have peak sensitivities in different parts of the visible spectrum. The second stage begins at the level of the retina and extends through the lateral geniculate nucleus of the thalamus (LGN) to the cortex. Here, input from the cones is compared in at least three separate channels. Most models propose that the $S-(L+M)$ and L–M channels are chromatically opponent and a third channel sums input from the different cones to convey a luminance signal [1–3].

Psychophysical results have indicated the presence of channels that are tuned to colors that do not selectively activate either the $S-(L+M)$ or L–M opponent channels, but are instead tuned to chromaticities that vary along intermediate directions of color space [4–8]. Webster and Mollon [5,6] have demonstrated that after adapting to intermediate axes of an opponent, cone-based color space (scaled MBDKL [3,9]), subjects reported the largest loss in sensitivity along the adapted axis as well as a shift of the perceived hue away from the adapted axis toward the orthogonal axis. This is inconsistent with the three-channel-only model that would predict adaptation to the cardinal axes that is proportionate to their relative proximity to the adapting axis, resulting in the greatest loss in sensitivity along the closest cardinal axis rather than the adapted axis itself, and a change in perceived hue toward the least adapted cardinal axis rather than the orthogonal axis. The two-channel model also predicts that adaptation along axes functionally intermediate between the two cardinal axes should produce uniform adaption along all axes. The Webster and Mollon data do not support a two-channel model.

Physiological evidence also supports a multitiered processing model. Cells in the koniocellular (kLGN) and parvocellular (pLGN) layers of the LGN show tuning to chromaticities along the cardinal axes in color space [2,3]. However, these cells do not change their response properties after prolonged exposure to contrast [3], as opposed to cells in the magnocellular (mLGN) layers [10], and therefore cannot account for changes in perception following chromatic contrast adaptation. Likewise, color-responsive cells in the LGN are monocular, yet chromatic contrast adaptation appears to be a binocular process since intraocular transfer has been reliably demonstrated [6,11]. Furthermore, fMRI data from Engel and Furmanski [12] suggest that the responses of groups of color-responsive cells in primary visual cortex independently alter their activity after adaptation and closely follow reported shifts in perception. Single-unit recordings from monkey cortex have also demonstrated characteristics consistent with behavior and many cells appear to possess chromatic tuning that is most sensitive along noncardinal directions of color space [13–17]. In fact, it has been shown that cells in the visual cortex show preferred chromatic tuning that is distributed throughout the isoluminant plane. These cells could conceivably receive their input in the form of differently weighted signals from the earlier stage of processing defined by the S and L–M opponent channels [18]. Viewed together, the psychophysical and physiological data suggest that the neurological substrate for contrast adaptation is after the LGN, i.e., in the cortex.

Physiological responses measured by chromatic visual evoked potentials (crVEPs) have revealed signal attenuation along cardinal axes after long- and short-wavelength chromatic adaptation [19]. These data have demonstrated that the crVEP reveals color mechanisms that are selective at the opponent level, giving researchers and clinicians the ability to noninvasively isolate and examine processing in the S, L–M, and luminance channels separately. Preferential activation of these different channels has revealed responses with distinctive physical and temporal characteristics [19,20]. These characteristics change throughout life and can be altered in the presence of pathology. As a result, testing of the independent opponent channels has been employed as a tool to investigate the integrity of the human visual system beyond the retina (e.g., [21–27]) as well as its maturation and development [27–36]. In addition, it is possible that the crVEP also reflects selectivity not only for the cardinal mechanisms but also those tuned to intermediate directions found at the next stage of chromatic processing. If this is the case, then the crVEP could be capable of providing researchers and clinicians a window into the hierarchy of color processing that was otherwise only accessible via more invasive or expensive techniques, such as single-unit recordings or MR imaging. However, contrast adaptation along noncardinal axes has yet to be measured with the crVEP. The present study more fully investigates the organizational nature of chromatic sensitivity in the cortex as reflected in the crVEP by comparing responses to stimuli modulated along intermediate as well as cardinal axes before and after chromatic contrast adaptation. The results demonstrate selective adaptation along intermediate axes and suggest that the crVEP response includes activity from cells that are tuned to cardinal directions as well as higher-order, intermediate directions.

2. METHODS

A. Participants

crVEPs were obtained from nine participants, three males and six females, aged 19 to 37 years. Written informed consent was obtained following the tenets of Helsinki, and with approval of the Office of Human Research Protection of the University of Nevada, Reno. Normal color vision was verified using the Ishihara 38 plate test and an Oculus HMC anomaloscope.

B. Stimuli

The VEP stimuli were horizontal sinusoidal gratings of 1.0 cpd, generated by a VSG card (Cambridge Research Systems) and presented binocularly on a Sony Trinitron Multiscan 20 sc II monitor. The display size was 27° × 35° and was viewed from 57 cm. Stimuli were presented in an onset/offset timing sequence (100 ms on, 425 ms off) and were chosen to preferentially activate the two cardinal axes (0°–180° [L–M]; 90°–270° [S]) and two intermediate axes (45°–225°; 135°–315°) of a scaled version of the L–M and S equiluminant planes [6, 37] defined by the following equations:

$$\begin{aligned}\text{L–M contrast} &= (r_{mb} - 0.6568) \times 1955\\ \text{S–LM contrast} &= (b_{mb} - 0.01825) \times 5533\end{aligned} \tag{1}$$

The stimuli were modulated along a line from −60 to +60 in this space. Stimuli were equated for individual isoluminance [37] and the cone-based space was further scaled such that contrast along the L–M axis was set to be perceptually equivalent to that of the S cone stimulus [38] for each individual subject. Gratings with high contrast (±60 units in the color space above) were used for adapting and test stimuli. The patterns were modulated around 0.6568, 0.1825 in Macleod–Boynton space (illuminant C), with a mean luminance of 20 cd/m^2. The adaptation stimuli were identical to the VEP stimuli except that the patterns were reversed at 8 Hz rather than presented in an onset/offset mode. This mode of adaptation has been shown previously to be effective along the cardinal axes [17].

C. VEP Recording

VEPs were recorded using gold-plated Grass electrodes and Grass amplifiers via a National Instruments input/output board in a PC. Electrodes were fixed with conductive paste according to the International 10–20 system. The active electrode was placed at Oz, the reference at Fz, and the ground was clipped to the earlobe. Electrode impedance was kept below 10 kΩ at 30 Hz. Gross potentials were sampled at 500 Hz. Signals were amplified, 60 Hz (mains) filtered, digitally low-pass filtered (100 Hz), and averaged over 60 presentations.

D. Procedure

VEPs were recorded prior to and after adaptation to four axes in MBDKL color space; 0°–180°, 45°–225°, 90°–270°, and 135°–315°. Baseline VEPs to all four test axes were first recorded in random sequence before adaptation. Subjects then adapted to 8 Hz grating reversals along one axis for 2 min before VEPs were recorded to one presentation of each of the four axes in a random order. Participants were then readapted to the same grating reversals for 10 s before repeating random tests of all four axes. This process was repeated until 60 trials were recorded and averaged per test axis. Each of the four different adaptation conditions was run on separate days to avoid any influence of long-term adaptation.

3. RESULTS

Amplitude of the test signal was taken as the difference in voltage between the CII and CIII components of the crVEP waveform. An adaptation index was then calculated to normalize the amplitude differences between pre- and postadaptation conditions [(preadapt − postadapt)/(preadapt + postadapt)]. This produced a range wherein a positive value indicated reduced amplitude with adaptation and zero is no change. When adapted to a particular axis, amplitude is expected to be more attenuated when tested on the same axis than when tested on the orthogonal axis if the adaptation was selective for that axis. The least-squares error was calculated between the amplitude indices of each adaptation condition and the best-fitting ellipse with the major and minor axes constrained to the adapted axis and its orthogonal axis. As a result, an aspect ratio was obtained such that the denominator represented the best fit along the adapted axis and the numerator represented the best fit along the orthogonal axis. Figure 1 illustrates the adaptation effect along each test axis as well as the corresponding ellipse fit. As is clearly visible in these polar plots, adaptation selectively attenuates the VEP signal amplitude along the adapt axis significantly more than that along the orthogonal axis.

Raw amplitudes were also used to compare the mean differences between the preadaptation responses from all four axes. Among the two intermediate directions tested, stimuli modulated along the 135°–315° axis elicited higher amplitude overall than did stimuli modulated along the 45°–225° axis, suggesting some asymmetry between the two intermediate channels.

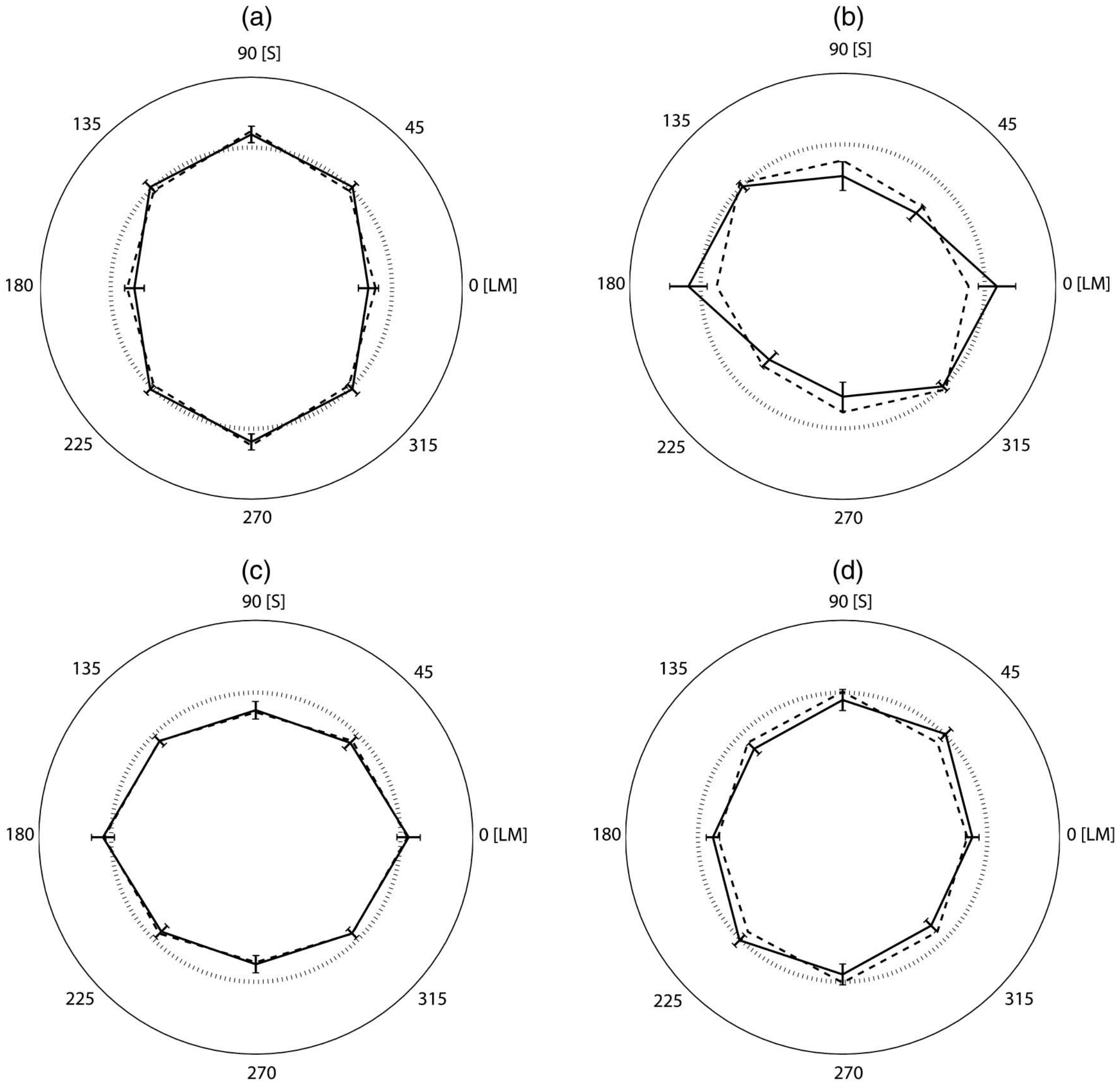

Fig. 1. Mean amplitude indices of pre- and postadaptation within the equiluminant plane. The inner solid line plots the coordinates of the test stimuli at each axis, while the heavy dashed line plots the least-squares ellipse fit, and the thin dashed line shows no adaptation effect. Error bars represent standard error of the means. Data points are reflected symmetrically. (a) 0°–180° adapting axis, (b) 45°–225° adapting axis, (c) 90°–270° adapting axis, (d) 135°–315° adapting axis.

A. Adapt 0°–180°

The ellipse best fit to the L–M adapt condition data had an aspect ratio of 1.27 (1.12/0.88), which was significantly different than a circle, $t(8) = 4.29$, $p < 0.0013$. T-tests also indicate that the test responses were more attenuated along the L–M axis than along the orthogonal axis (S), $t(8) = -2.11$, $p < 0.034$. Furthermore, the radius of the fit along the L–M axis was significantly different than 1, $t(8) = 4.58$, $p < 0.00009$, indicating adaptation. The radius along the S axis was also significantly different from 1, $t = 2.65$, $p < 0.0147$, but, as can be seen in Fig. 1, sensitivity along the S axis was increased rather than adapted, indicating that adaptation was selective along the L–M axis.

B. Adapt 45°–225°

The ellipse best fit to the 45°–225° adapt condition data had an aspect ratio of 1.24 (1.03/0.83), which was also significantly different than a circle, $t(8) = -2.30$, $p < 0.0251$. T-tests also indicate that the radius of the fit along the adapted axis was significantly shorter than that along the orthogonal axis (135°–315°), $t(8) = -2.34$, $p < 0.02389$, demonstrating that sensitivity along the 45°–225° axis was more adapted than that along the orthogonal axis, i.e., selective tuning along intermediate color directions. Furthermore, the radius of the fit along the adapt axis was significantly different from 1, $t = 2.34$, $p < .0239$, and that along the orthogonal axis (135°–315°) was not, $t = 0.45$, $p < 0.3325$. These data indicate that adaptation was selective along the 45°–225° axis.

C. Adapt 90°–270°

The ellipse best fit to the S adapt condition data had an aspect ratio of 1.27 (1.07/0.86). T-tests also indicate that the radius of the fit along the adapted axis was significantly shorter than that along the orthogonal axis (L–M), $t(8) = -2.78$, $p < 0.01181$, demonstrating that sensitivity along the S axis was more adapted than that along the L–M axis, indicating selective tuning along the S axis. Furthermore, the radius of the fit along the adapted axis was significantly different

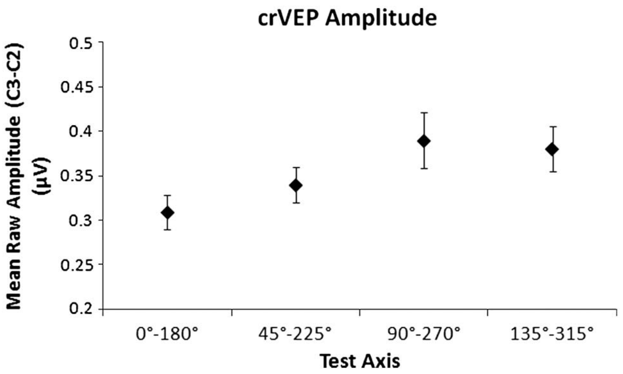

Fig. 2. Mean raw preadaptation amplitudes (CIII-CII) per test condition. Error bars represent standard error of the mean.

from 1, $t = 3.69$, $p < 0.0031$, and that along the orthogonal axis (L–M) was not, $t = 0.16$, $p < 0.4387$.

D. Adapt 135°–315°

The ellipse best fit to the 135°–315° adapt condition data had an aspect ratio of 1.18 (1.01/0.87). T-tests also indicate that the radius of the fit along the adapted axis was significantly shorter than that along the orthogonal axis (45°–225°), $t(8) = -2.21$, $p < 0.02889$, demonstrating that sensitivity along the 135°–315° axis was more adapted than that along the orthogonal axis, indicating selective tuning along intermediate color directions. Furthermore, the radius of the fit along the adapt axis was significantly different from 1, $t = 2.62$, $p < 0.0153$, and that along the orthogonal axis (45°–225°) was not, $t = 0.16$, $p < 0.4387$.

4. DISCUSSION

The CIII-CII amplitude differences between pre- and postadaptation appear to demonstrate at least two additional channels whose sensitivities lie between those of the cardinal directions in color space. Adaptation to either of the intermediate color directions resulted in significantly more adaptation along the adapted axis than the orthogonal axis. If cells in the S and L–M channels were the only contributors to the crVEP, then it would be expected that adaptation along either intermediate axis would essentially be synonymous with concurrent adaptation along both the S and L–M axes. This is because it is assumed that responses from stimuli along the two intermediate axes would receive sizable inputs from both the fundamental S and L–M channels [11]. The two-channel model also predicts that adaptation along either intermediate axis would result in similar signal attenuation along its orthogonal axis as well, since both receive their input from the same two sources. Instead, the data suggest that the crVEP reveals the presence of independently adaptable intermediate channels in addition to those tuned to the cardinal directions of color space. Previous research has identified cells with peak sensitivities lying between the cardinal directions in V1 [39,40], V2 [13], and V4 [41] that could easily contribute to the crVEP response.

The averaged raw amplitudes of the responses in the unadapted condition are shown in Fig. 2. There are two interesting features of these data. The first is that for the present stimulus conditions, equation by psychophysical contrast matching along the cardinal axes produces responses that are slightly larger for the S axis than those for the L–M axis. This is consistent with prior reports (e.g., [19]). The second feature is that a difference in overall preadaption amplitude was also observed between tests of the intermediate channels. As can be seen in Fig. 2., the 45°–225° preadapt condition has significantly larger amplitude than the 135°–315°, $t = 2.26$, $p < 0.01515$. These results are in agreement with Goddard, Mannion, McDonald, Solomon and Clifford [40] who found a strong cortical bias for stimuli modulated along a lime green/magenta axis (45°–225°) over the orange/cyan axis (135°–315°) in the BOLD signal as early as V1. These data indicate that there is either a greater population of neurons responsive to the 45°–225° direction or that these neurons are just more responsive than those tuned to the orthogonal direction. Other results from single-unit recordings in macaque [42,43] and psychophysical data [44] suggest the opposite; the 135°–315° direction is slightly biased indicating a need for further investigation. The present results suggest that future applications of the crVEP may be expanded beyond that of the opponent channels to include the next level of color processing.

REFERENCES

1. R. L. De Valois and K. K. De Valois, “A multi-stage color model,” Vision Res. **33**, 1053–1065 (1993).
2. R. L. De Valois, J. Abramov, and G. H. Jacobs, “Analysis of response patterns of LGN cells,” J. Opt. Soc. Am. **56**, 966–977 (1966).
3. A. M. Derrington, J. Krauskopf, and P. Lenni, “Chromatic mechanisms in lateral geniculate nucleus of macaque,” J. Physiol. **357**, 241–265 (1984).
4. J. Krauskopf, D. R. Williams, M. B. Mandler, and A. M. Brown, “Higher order color mechanisms,” Vision Res. **26**, 23–32 (1986).
5. M. A. Webster and J. D. Mollon, “Changes in colour appearance following post-receptoral adaptation,” Nature **349**, 235–238 (1991).
6. M. A. Webster and J. D. Mollon, “The influence of contrast adaptation on color appearance,” Vision Res. **34**, 1993–2020 (1994).
7. K. Ichiro, “Aftereffect of contrast adaptation to a chromatic notched-noise stimulus,” J. Opt. Soc. Am. A **24**, 1858–1872 (2007).
8. Y. Mizokami and M. A. Webster, “Chromatic and contrast selectivity in color contrast adaptation,” Vis. Neurosci. **21**, 359–363 (2004).
9. D. I. A. MacLeod and R. M. Boynton, “Chromaticity diagram showing cone excitation by stimuli of equal luminance,” J. Opt. Soc. Am. **69**, 1183–1186 (1979).
10. S. G. Solomon, J. W. Peirce, N. T. Dhruv, and P. Lennie, “Profound contrast adaptation early in the visual pathway,” Neuron **42**, 155–162 (2004).
11. J. Krauskopf, D. R. Williams, and D. W. Heely, “Cardinal directions of color space,” Vision Res. **22**, 1123–1131 (1982).

12. S. A. Engel and C. S. Furmanski, “Selective adaptation to color contrast in human primary visual cortex,” J. Neurosci. **21**, 3949–3954 (2001).
13. A. Hanazawa, H. Komatsu, and I. Murakami, “Neural selectivity for hue and saturation of colour in the primary visual cortex of the monkey,” Eur. J. Neurosci. **12**, 1753–1763 (2000).
14. D. C. Kiper, S. B. Fenstemaker, and K. R. Gegenfurtner, “Chromatic properties of neurons in macaque area V2,” Vis. Neurosci. **14**, 1061–1072 (1997).
15. T. Matsumora, K. Koida, and H. Komatsu, “Relationship between color discrimination and neural responses in inferior temporal cortex of monkey,” J. Neurophysiol. **100**, 3361–3374 (2008).
16. P. Lennie, J. Krauskopf, and G. Sclar, “Chromatic mechanisms in striate cortex of Macaque,” J. Neurosci. **10**, 649–669 (1990).
17. H. Lim, Y. Wang, Y. Xiao, M. Hu, and D. J. Felleman, “Organization of hue selectivity in macaque V2 thin stripes,” J. Neurophysiol. **102**, 2603–2615 (2009).
18. C. Tailby, S. G. Solomon, N. T. Dhruv, and P. Lennie, “Habituation reveals fundamental chromatic mechanisms in striate cortex of macaque,” J. Neurosci. **28**, 1131–1139 (2008).
19. J. Rabin, E. Switkes, M. A. Crognlae, M. E. Schneck, and A. J. Adams, “Visual evoked potentials in three-dimensional color space: correlates of spatiochromatic processing,” Vision Res. **34**, 2657–2671 (1994).
20. C. Gerth, P. B. Delahunt, M. A. Crognale, and J. S. Werner, “Topography of the chromatic pattern-onset VEP,” J. Vision **3**, 171–182 (2003).
21. N. Accornero, B. Gregori, E. Galié, A. De Feo, and R. Agnesi, “A new color VEP procedure discloses asymptomatic visual impairments in optic neuritis and glaucoma suspects,” Acta Neurologica Scandinavica **102**, 258–263 (2000).
22. M. A. Crognale, J. Rabin, E. Switkes, and A. J. Adams, “Selective loss of S pathway sensitivity in central serous choroidopathy revealed by spatio-chromatic visual evoked cortical potentials (VECP),” *Color Vision Deficiencies XI*, Documenta Ophthalmologica Proceedings Series (Kluwer, Dordrecht, 1993), pp. 229–239.
23. V. Porciatti, E. Bartolo, M. Nardi, and A. Fiorentini, “Responses to chromatic and luminance contrast in glaucoma: a psychophysical and electrophysiological study,” Vision Res. **37**, 1975–1987 (1997).
24. M. A. Crognale, E. Switkes, J. Rabin, M. E. Schneck, G. Haegerström-Portnoy, and A. J. Adams, “Application of the spatio-chromatic visual evoked potential to detection of congenital and acquired color deficiencies,” J. Opt. Soc. Am. **10**, 1818–1825 (1993).
25. M. E. Schneck, B. F. Fortune, M. A. Crognale, E. Switkes, and A. J. Adams, “Influence of blood glucose level on chromatic VEP’s in type I diabetes,” in *Vision Science and its Applications*, Vol. **1**, 1996 OSA Technical Digest Series (Optical Society of America, Washington, D.C.), pp. 38–42 (1996).
26. M. E. Schneck, E. Lee, B. F. Fortune, E. Switkes, M. A. Crognale, and A. J. Adam, “Spatio-chromatic VEPs in recovered optic neuritis and multiple sclerosis,” *Color Vision Deficiencies XIII*, Documenta Ophthalmologica Proceedings Series (Kluwer, Dordrecht, 1997), pp. 179–185.
27. C. M. Suttle and R. Lloyd, “Chromatic and achromatic transient VEPs in adults with Down syndrome.” Ophthal. Physiol. Opt. **25**, 501–513 (2005).
28. M. Y. Boon, C. M. Suttle, and S. J. Dain, “Transient VEP and psychophysical chromatic contrast thresholds in children and adults.” Vision Res. **47**, 2124–2133 (2007).
29. J. J. Brecelj, M. M. Štrucl, I. I. Zidar, and M. M. Tekavčič-Pompe, “Pattern ERG and VEP maturation in schoolchildren.” Clinical Neurophysiology **113**, 1764–1770 (2002).
30. M. A. Crognale, “Development, maturation, and aging of chromatic visual pathways: VEP results.” J. Vision **2**, 438–450 (2002).
31. M. A. Crognale, J. P. Kelly, S. Chang, A. H. Weiss, and D. Y. Teller, “Development of pattern visual evoked potentials: Longitudinal measurements in human infants.” Optom. Vis. Sci. **74**, 808–815 (1997).
32. M. A. Crognale, J. P. Kelly, A. Weiss, and D. Y. Teller, “Development of the spatio-chromatic visual evoked potential (VEP): A longitudinal study.” Vision Res. **38**, 3283–3292 (1998).
33. J. W. Page and M. A. Crognale, “Differential aging of chromatic and achromatic visual pathways: behavior and electrophysiology.” Vision Res. **45**, 1481–1489 (2005).
34. M. Pompe, B. Kranjc, and J. Brecelj, “Visual evoked potentials to red-green stimulation in schoolchildren.” Vis. Neurosci. **23**, 447–451 (2006).
35. C. M. Suttle, S. J. Anderson, and F. A. Graham, “A longitudinal study of visual evoked responses to tritan stimuli in human infants.” Optom. Vis. Sci. **74**, 717–725 (1997).
36. M. M. Tekavčič-Pompe, B. S. Kranjc, and J. J. Brecelj, “The study of chromatic and achromatic VEP in the first year of life,” Acta Ophthalm. **87**, 0 (2009).
37. S. Anstis and P. Cavanagh, “A minimum motion technique for judging equiluminance,” in*Colour Vision* (J. D. Mollon and L. T. Sharp, eds.) (Academic, London, 1983) pp. 155–166.
38. E. Switkes and M. A. Crognale, “Comparison of color and luminance contrast: apples versus oranges?,” Vision Res. **39**, 1823–1831 (1999).
39. T. Wachtler, T. J. Sejnowski, and T. D. Albright, “Representation of color stimuli in awake macaque primary visual cortex,” Neuron **37**, 681–691 (2003).
40. E. Goddard, D. J. Mannion, J. S. McDonald, S. G. Solomon, and C. W. G. Clifford, “Combination of subcortical color channels in human visual cortex,” J. Vision **10**, 25 (2010).
41. S. Zeki, “The representation of colours in the cerebral cortex,” Nature **284**, 412–418 (1980).
42. B. R. Conway, “Spatial structure of cone inputs to color cells in alert macaque primary visual cortex (V-1),” J. Neurosci. **21**, 2768–2783 (2001).
43. S. G. Solomon and P. L. Lennie, “Chromatic gain controls in visual cortical neurons.” J. Neurosci. **25**, 4779–4792 (2005).
44. J. Krauskopf and K. Gegenfurtner, “Color discrimination and adaptation,” Vision Res. **32**, 2165–2175 (1992).